SUPPLEMENTAL TABLES

Table S1. A list of genes that are differentially transcribed between Myt1^{+}Neurog3^{+} and Myt1^{-}Neurog3^{+} progenitor cells. Related to Figure 1. Only genes with a *p* value below 0.05 were listed. Note that for each gene, the average and SEM were provided, together with the *p*-value.

Table S2. Lists of genes associated with DMRs between *Neurog3*$^{eGFP/eGFP}$ null and *Neurog3*$^{eGFP/+}$ heterozygous cell populations. Related to Figure 5. Official genes names were presented.

Table S3. The number of cells counted for all quantification processes. Related to Figure 2, 4, 6. The corresponding panel was noted in each set of data.

SUPPLEMENTARY FIGURES

Figure S1. The heterogeneity of Neurog3+ cells in the developing pancreas. Related to Figure 1. (A, B) Co-immunostainning of Myt1 and Neurog3 in E10.5 and E14.5 embryonic pancreata. Arrowheads, single Ngn3^{+} cells. Arrows, double Neurog3^{+}TF^{+} cells. (C) Quantification of Neurog3^{+} cells that co-express Myt1, Pax6, and Pdx1 at different stages. Error bars, SEM. (D, E) Co-immunostainning of Pax6 or Pdx1 with Neurog3 in E14.5 pancreata. Arrowheads, single Ngn3+ cells. Arrows, double Neurog+TF+ cells. Scale bars=20 μm. (F) Gating strategy for flow sorting *eGFP*-expressing cells for downstream scRNA-seq analysis. (G) Evaluation of doublet rate of scRNA-seq experiments by co-encapsulating human K562 cells with E14.5 mouse pancreatic cells. Mouse (Y-axis) or human (X-axis) β-actin transcript counts are plotted for each filtered barcode representing a cell. (H) t-SNE analysis of 1,635 GFP-sorted cells from two biological replicate experiments. Black and grey

represent each replicate and the degree of mixing between the two colors indicates the relative absence of batch effects. (I1-I5) Overlays of non-endocrine cell lineage specific gene markers on t-SNE, with identified populations manually annotated. Overlays represent gene expression levels on a variance normalized (Asinh) scale. (J1-5) Overlays of endocrine cell-type specific gene markers on t-SNE. Overlays represent gene expression levels on a variance normalized (Asinh) scale. There were not enough intermediate cell states connecting *Sst*-expressing cell states to the general endocrine cluster (J5). The general endocrine population was gated for downstream p-Creode analysis of endocrine differentiation.

Figure S2. *nCre* and *cCre* expression-based lineage tracing. Related to Figure 2. (A, B) Insulin staining and β-cell area quantification in control (no transgene) and *Myt1*^{cCre}*; Neurog3*^{nCre}*; Ai9* (*MNA*) compound mice. (C) Random blood glucose of newly-born control and *MNA* mice. (D) Intraperitoneal glucose tolerance test of control and *MNA* mice 6-week after birth. (E-G) Combinatorial lineage tracing of Myt1^{+}Neurog3^{+} cells in P1 *Myt1*^{cCre}*; Neurog3*$^{tg\text{-}nCre}$*; Ai9* mice. Note that *Neurog3*$^{tg\text{-}nCre}$ is a BAC-based transgene, so that its presence does not interfere with Neurog3 production in progenitor cells. (E, F) Representative images of Ins, Gcg, and Sst co-staining with tdTomato production (red). (G) Quantification of lineage marked cells in P1 *Myt1*^{cCre}*; Neurog3*$^{tg\text{-}nCre}$*; Ai9* mice (n=4-5). Scale bar in F=20 μm.

Figure S3: Supervised analysis of *Myt1*$^{+}$ and *Myt1*$^{-}$ endocrine progenitor cells using PLSDA on scRNA-seq data. Related to Figure 3. (A) Gating strategy for *Myt1*$^{+}$ and *Myt1*$^{-}$

endocrine progenitor cells. Endocrine progenitor cells were gated from the general endocrine population in Figure S1 for cells that do not express differentiated cell product genes, such as *Ins1*, *Gcg*, *Ghrl*, *Ppy*, *Sst*, resulting in 550 total endocrine progenitor cells. Progenitors were further gated for *Myt1* positivity (151 cells – 27%) and negativity (399 cells – 73%) for downstream PLSDA analysis. (B) Variance captured of the PLSDA model constructed from $Myt1^{+}$ and $Myt1^{-}$ endocrine progenitor cells as a function of the number of latent variables included. (C) Calibration (cal) and cross-validation (CV) error of the PLSDA model as a function of the number of latent variables included. (D) List of the top 20 biological processes. Red font highlights the epigenetic-based processes. (E, F) t-SNE overlay of *Arx* and *Pax4* expression in flow-sorted *Neurog3*-expressing cells. Note the differential temporal expression of *Arx* (E) and *Pax4* (F) within the endocrine lineage.

Figure S4. Epigenetic manipulation on islet-cell type allocation. Related to Figure 4.

(A-G) E12.5 pancreatic buds cultured five days in DMSO or 5 μM Adox were used for all assays. (A-D) Neurog3, Myt1, and Pdx1 production in pancreatic buds in 5 μM Adox (A, B) or DMSO (C, D). (E-G) Ins and Gcg staining and quantification. (H-N) Effects of AzaC on islet cell allocation. E12.5 pancreatic buds cultured five days in DMSO or 2 μM AzaC were used for all assays. (H-J) MafB/Gcg production in pancreatic buds. (J) Real-time RT-PCR of *Arx*/*Gcg* transcription in pancreatic buds (higher ΔCT means higher expression). (K, L) Assays for cleaved Caspase3 (Cas3), an apoptotic marker, in cultured pancreatic buds. (M, N) Cell proliferation in cultured pancreatic buds. (O-Q) Effects of *Dnmt3b* overexpression on islet cell allocation**.** TetO-based *Dnmt3b* overexpression ($Dnmt3b^{OE}$) was driven by *Pdx1cre* in combination with $Rosa26^{rTTA\text{-}ires\text{-}eGFP}$, which resulted in the expression of rTTA in most

pancreatic cells. Dox was added from E10.5 until tissue collection at E16.5. Scale bars in all panels, 20 μm.

Figure S5. Methylation status in CpG islands of pancreatic progenitors. Related to Figure 5. *Neurog3* expressing cells sorted from E14.5 *Neurog3*$^{eGFP/+}$ or *Neurog3*$^{eGFP/eGFP}$ pancreata were used for DNA isolation and bisulfite sequencing for PCR (A) or sequencing (B, C). (A) Methylation CpG islands of *Pax4, Pax6, Pdx1, Nkx2.2,* and *Nkx6.1*, assayed via PCR-sequencing. The locations of the reported CpG islands were marked by their relative position to the transcription initiation site. Black circles indicate methylated CpG dinucleotide. (B, C) Some DMRs from genome-wide methylome assays. (B) Differentially Methylated Regions (DMRs) in *Ngn3* null and Heterozygous cells. Note that the majority of the DMRs were hypomethylated in the Ngn3 heterozygous cells. (C) The relative locations of DMRs relative most genes.

Figure S6. Methylation status near the *Nkx6.1* and *Arx* loci. Related to Figure 5. (A) Locations of several differentially methylated regions (DMRs, red rectangles) ~60 kilo-bases 3' to *Nkx6.1* between Ngn3-heterozygous (het) and null cells (E14.5). The hypomethylated regions (HMRs) were annotated with grey rectangles above each track. (B) The methylation states near the *Nkx6.1* transcription units. The CpG island examined via PCR-based sequencing, 5' end of *Nkx6.1* transcript, was marked with green rectangle. (C, D) Methylation states near *Arx* locus, in Ngn3 het and null cells. The green rectangle indicates the location of UR2.

Figure S7: Transcriptomic homogeneity of the E14.5 *Neurog3*$^{eGFP/eGFP}$ pancreas. Related to Figure 7.

t-SNE analysis of scRNA-seq data generated from E14.5 flow-sorted *Neurog3*$^{eGFP/eGFP}$ cells overlaid with cell lineage gene markers (A-C), *Neurog3*-dependent genes (D-F), *Neurog3*-independent genes (G), and genes for epigenetic modifying enzymes (H-L). (C) CD68 marks the presence of immune cells within flow-sorted GFP+ cells. Overlays represent gene expression levels on a variance normalized (Asinh) scale.

Figure S1

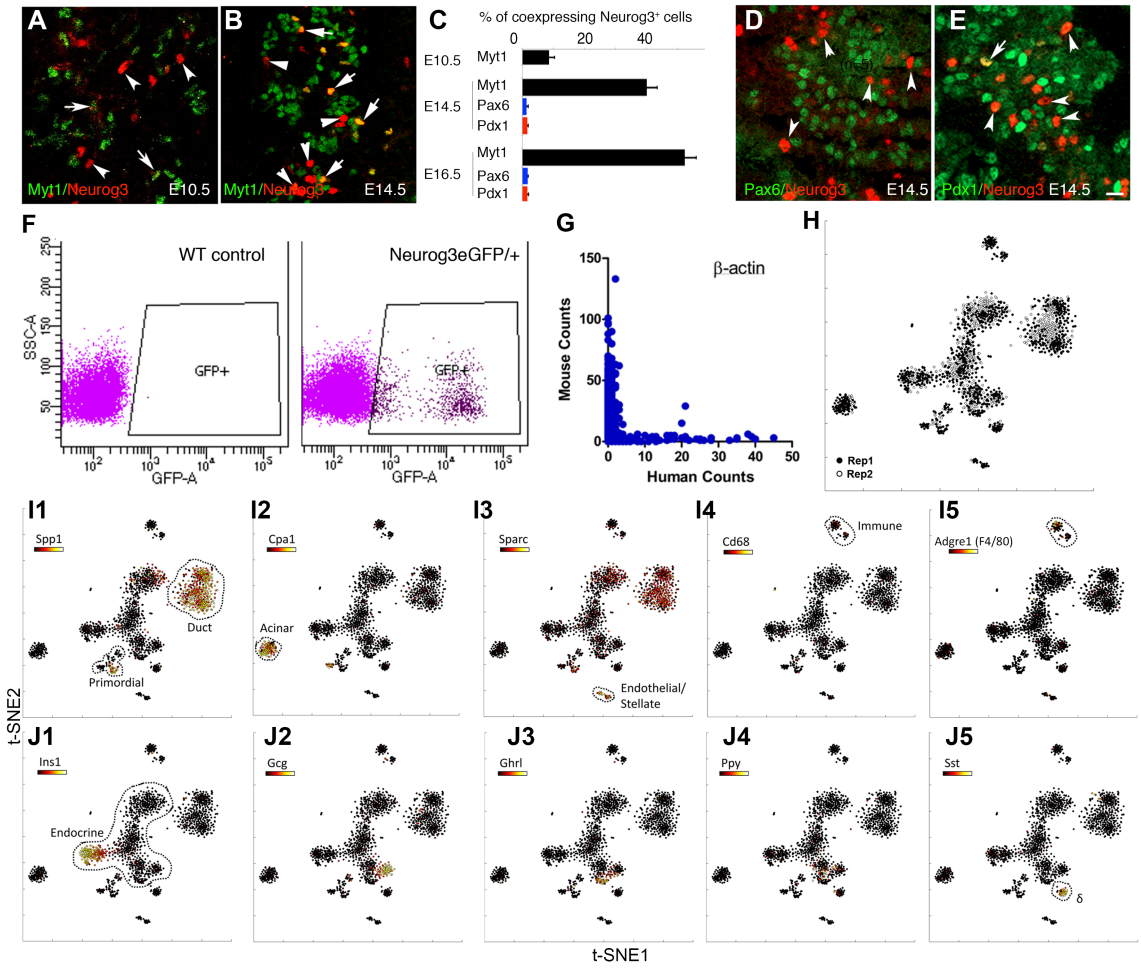
A
Myt1/Neurog3
E10.5
B
Myt1/Neurog3
E14.5
C
% of coexpressing Neurog3+ cells
0
20
40
E10.5
Myt1
E14.5
Myt1
Pax6
Pdx1
E16.5
Myt1
Pax6
Pdx1
D
Pax6/Neurog3
E14.5
E
Pdx1/Neurog3 E14.5
F
WT control
Neurog3eGFP/+
SSC-A
GFP+
GFP-A
G
β-actin
Mouse Counts
Human Counts
H
Rep1
Rep2
I1
Spp1
Duct
Primordial
I2
Cpa1
Acinar
I3
Sparc
Endothelial/
Stellate
I4
Cd68
Immune
I5
Adgre1 (F4/80)
J1
Ins1
Endocrine
J2
Gcg
J3
Ghrl
J4
Ppy
J5
Sst
δ
t-SNE2
t-SNE1

Figure S2

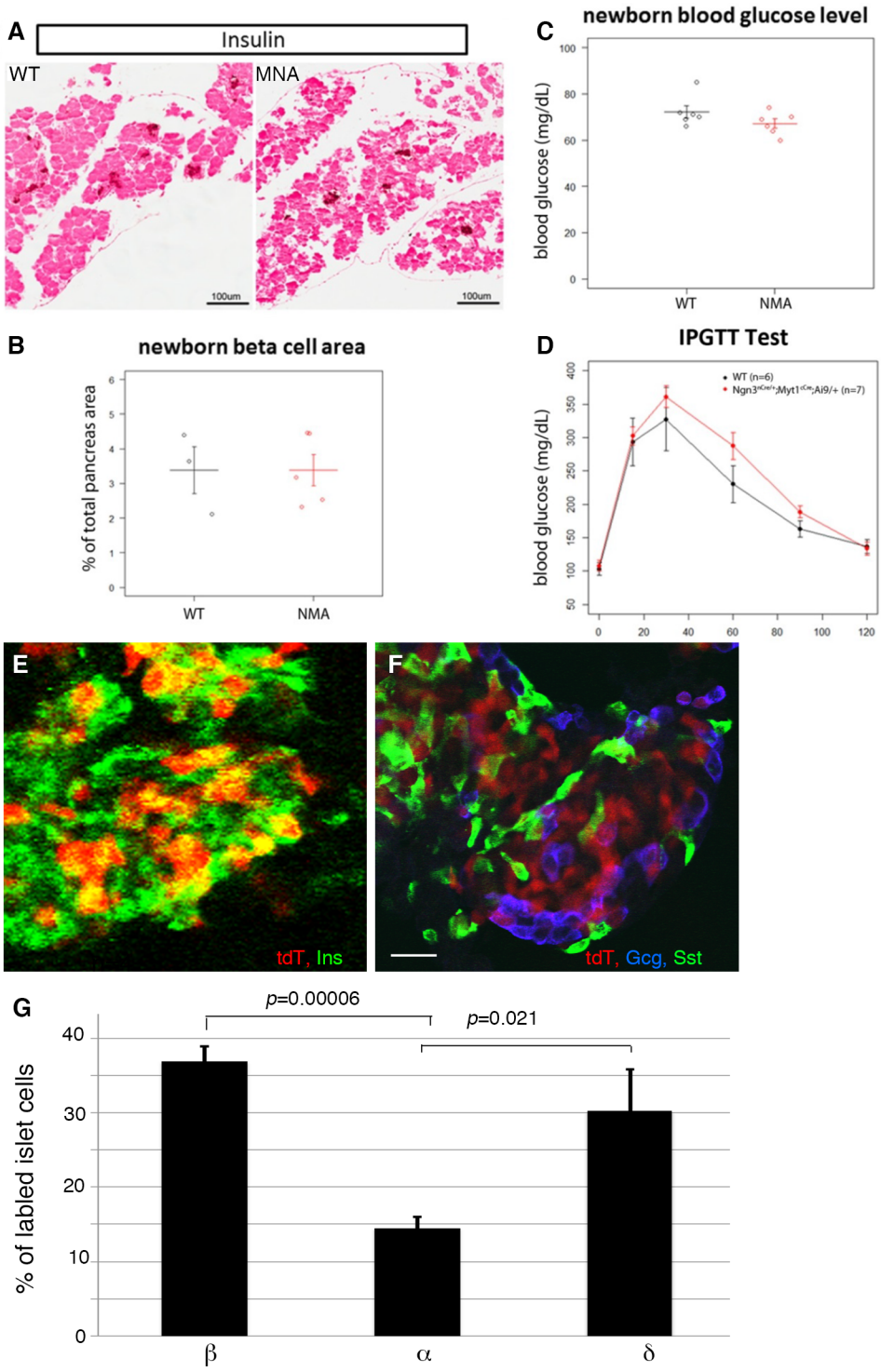
A
Insulin
WT
MNA
100um
100um
B
newborn beta cell area
% of total pancreas area
WT
NMA
C
newborn blood glucose level
blood glucose (mg/dL)
WT
NMA
D
IPGTT Test
blood glucose (mg/dL)
WT (n=6)
Ngn3iCre/+;Myt1iCre;Ai9/+ (n=7)
E
tdT, Ins
F
tdT, Gcg, Sst
G
p=0.00006
p=0.021
% of labled islet cells
β
α
δ

Figure S3

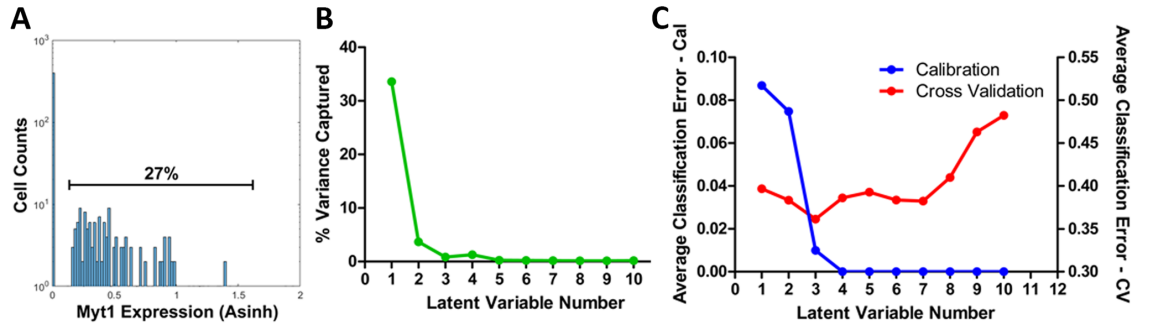

D

Ranked by Over-Representation in Myt1+ Progenitor Cells

Name	NES	p-value
CARD_MIR302A_TARGETS	2.146262	0
REACTOME_PEPTIDE_CHAIN_ELONGATION	2.144373	0
REACTOME_TRANSLATION	2.117292	0
BILANGES_SERUM_AND_RAPAMYCIN_SENSITIVE_GENES	2.115847	0
REACTOME_3_UTR_MEDIATED_TRANSLATIONAL_REGULATION	2.108974	0
REACTOME_ACTIVATION_OF_THE_MRNA_UPON_BINDING_OF_THE_CAP_BIND	2.095533	0.001658
KEGG_RIBOSOME	2.085503	0
BILANGES_SERUM_RESPONSE_TRANSLATION	2.065363	0
REACTOME_METABOLISM_OF_MRNA	2.061899	0
REACTOME_INFLUENZA_VIRAL_RNA_TRANSCRIPTION_AND_REPLICATION	2.044164	0
REACTOME_NONSENSE_MEDIATED_DECAY_ENHANCED_BY_THE_EXON_JUNCT	2.038317	0
MODY_HIPPOCAMPUS_PRENATAL	2.036073	0
REACTOME_METABOLISM_OF_RNA	2.035289	0
REACTOME_INFLUENZA_LIFE_CYCLE	2.005113	0
JISON_SICKLE_CELL_DISEASE_DN	2.004642	0
REACTOME_FORMATION_OF_THE_TERNARY_COMPLEX_AND_SUBSEQUENTLY	1.984259	0.001739
SCHLESINGER_H3K27ME3_IN_NORMAL_AND_METHYLATED_IN_CANCER	1.970417	0
REACTOME_SRP_DEPENDENT_COTRANSLATIONAL_PROTEIN_TARGETING_TO_M	1.964618	0
HSIAO_HOUSEKEEPING_GENES	1.961317	0
LEE_AGING_MUSCLE_UP	1.953731	0

Ranked by p-value of Change in Myt1+ Cells

NAME	NES	p-value
BILANGES_SERUM_RESPONSE_TRANSLATION	1.682421	0
TIEN_INTESTINE_PROBIOTICS_6HR_UP	1.677463	0
MYLLYKANGAS_AMPLIFICATION_HOT_SPOT_17	1.672686	0.002039
KIM_HYPOXIA	1.663031	0.001006
KEGG_O_GLYCAN_BIOSYNTHESIS	1.64849	0.00503
SATO_SILENCED_EPIGENETICALLY_IN_PANCREATIC_CANCER	1.637171	0.002002
VALK_AML_CLUSTER_2	1.635628	0.005045
ST_GRANULE_CELL_SURVIVAL_PATHWAY	1.613056	0.00503
LU_TUMOR_ENDOTHELIAL_MARKERS_UP	1.611025	0.007121
REACTOME_IL_RECEPTOR_SHC_SIGNALING	1.605915	0.006018
JOHNSTONE_PARVB_TARGETS_1_DN	1.59415	0
HWANG_PROSTATE_CANCER_MARKERS	1.586541	0.00603
SPIRA_SMOKERS_LUNG_CANCER_UP	1.58324	0.003
PID_WNT_NONCANONICAL_PATHWAY	1.57197	0.005005
POMEROY_MEDULLOBLASTOMA_PROGNOSIS_DN	1.571185	0.004
DORN_ADENOVIRUS_INFECTION_12HR_UP	1.569836	0.00603
BIOCARTA_BIOPEPTIDES_PATHWAY	1.56631	0.004
GENTILE_UV_RESPONSE_CLUSTER_D7	1.565343	0.006018
OUYANG_PROSTATE_CANCER_PROGRESSION_DN	1.56488	0.015244
DORN_ADENOVIRUS_INFECTION_24HR_DN	1.562333	0.003

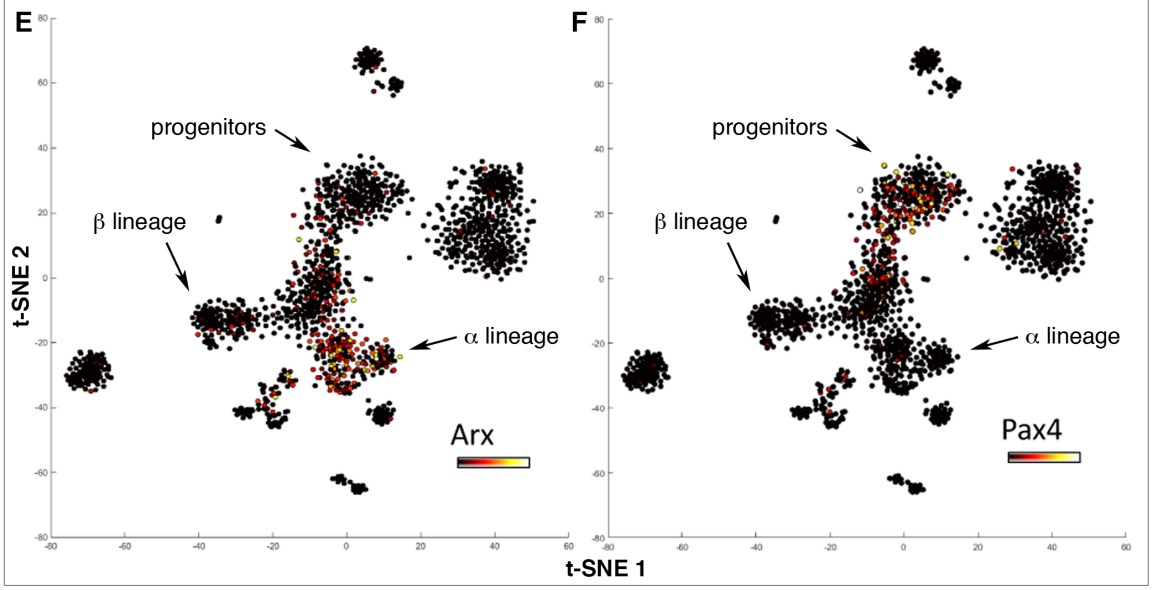

Figure S4

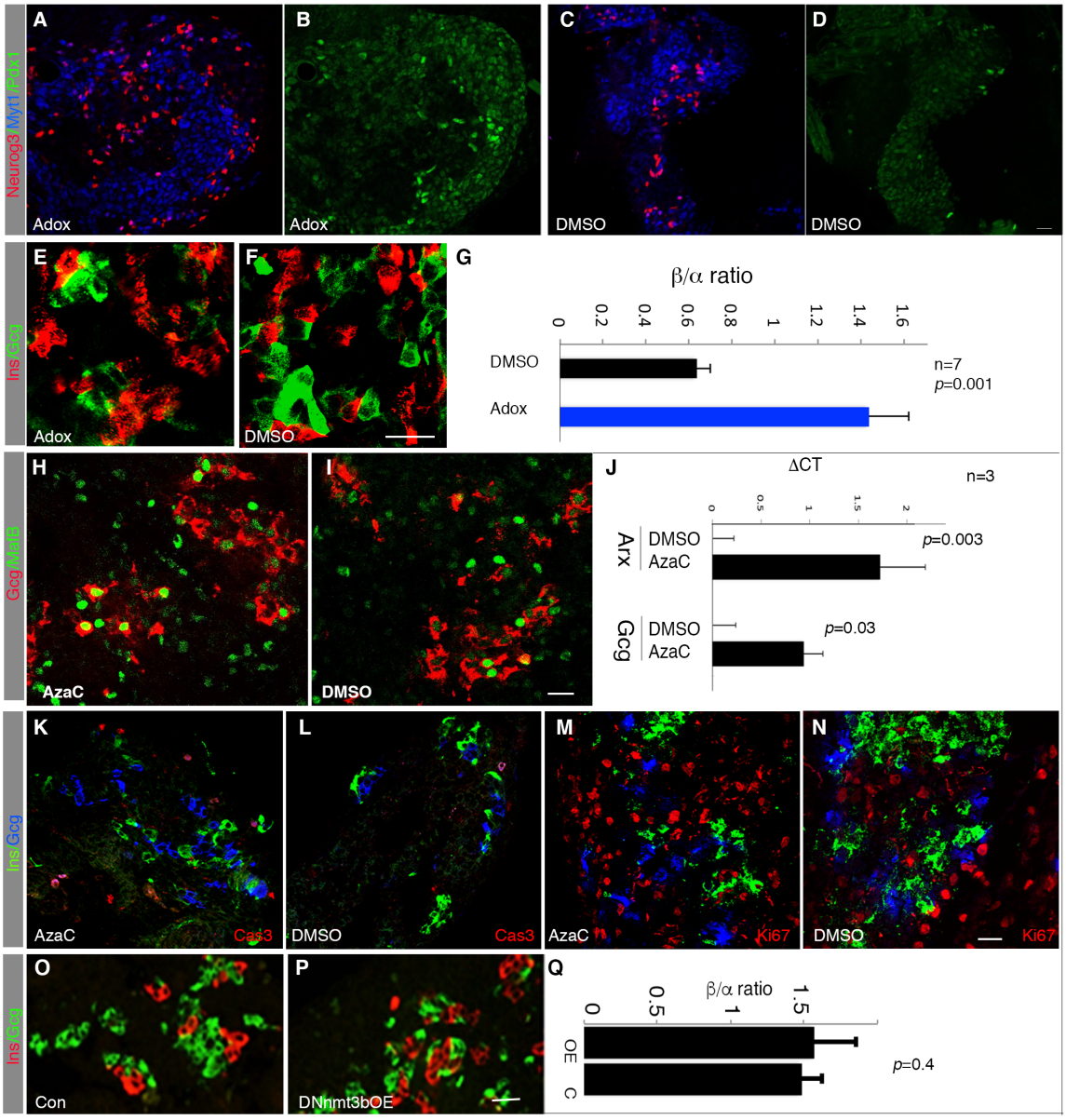
A
B
C
D
Neurog3 Myt1 Pdx1
Adox
Adox
DMSO
DMSO
E
F
G
Ins Gcg
Adox
DMSO
β/α ratio
0
0.2
0.4
0.6
0.8
1
1.2
1.4
1.6
DMSO
Adox
n=7
p=0.001
H
I
J
Gcg MafB
AzaC
DMSO
ΔCT
n=3
0
0.5
1
1.5
2
Arx
DMSO
AzaC
p=0.003
Gcg
DMSO
AzaC
p=0.03
K
L
M
N
Ins Gcg
AzaC
Cas3
DMSO
Cas3
AzaC
Ki67
DMSO
Ki67
O
P
Q
Ins Gcg
Con
DNnmt3bOE
β/α ratio
0
0.5
1
1.5
OE
C
p=0.4

Figure S5

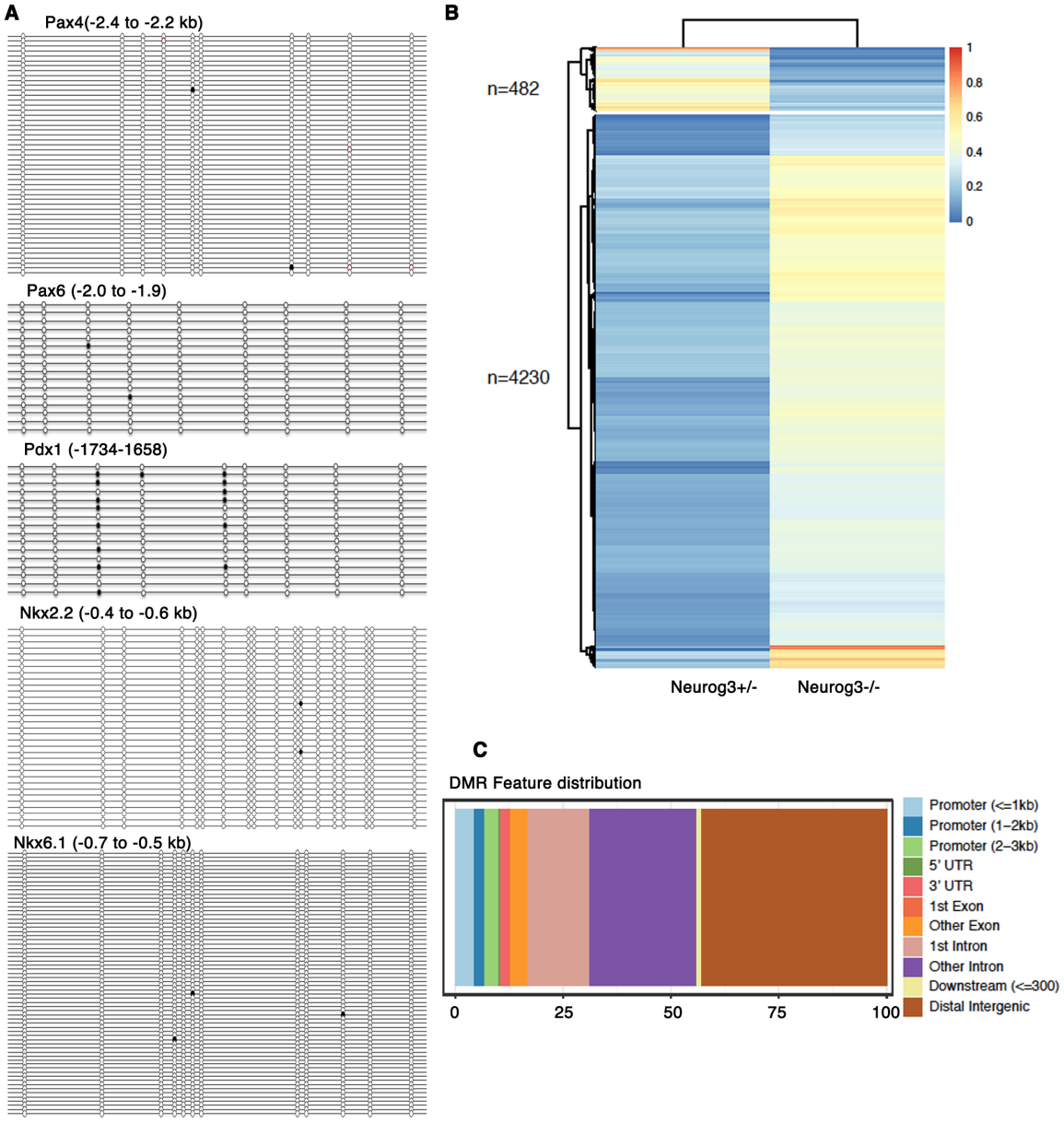
A
Pax4(-2.4 to -2.2 kb)
Pax6 (-2.0 to -1.9)
Pdx1 (-1734-1658)
Nkx2.2 (-0.4 to -0.6 kb)
Nkx6.1 (-0.7 to -0.5 kb)
B
n=482
n=4230
1
0.8
0.6
0.4
0.2
0
Neurog3+/-
Neurog3-/-
C
DMR Feature distribution
Promoter (<=1kb)
Promoter (1–2kb)
Promoter (2–3kb)
5' UTR
3' UTR
1st Exon
Other Exon
1st Intron
Other Intron
Downstream (<=300)
Distal Intergenic
0
25
50
75
100

Figure S6

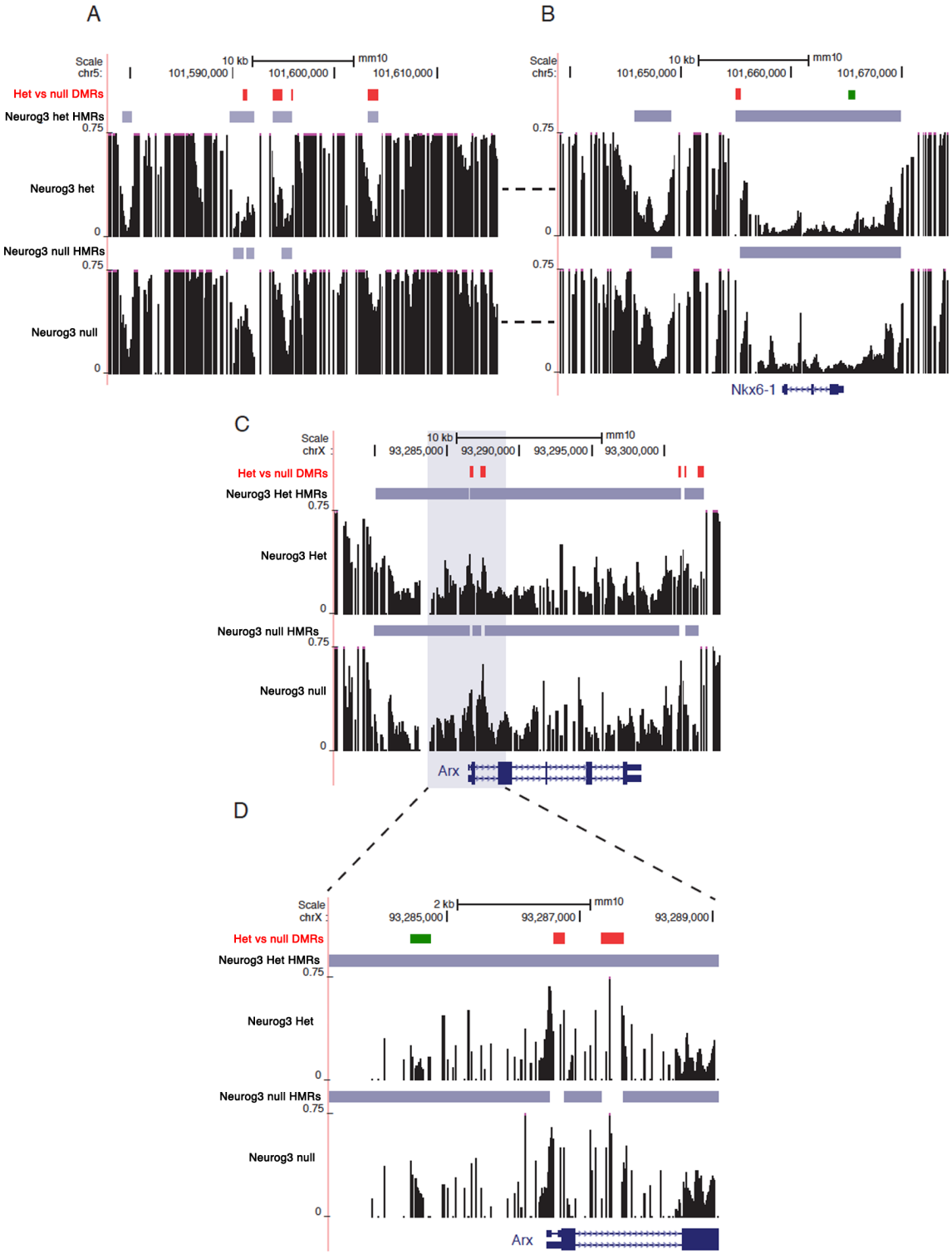
A
B
Scale
chr5:
10 kb
mm10
101,590,000
101,600,000
101,610,000
101,650,000
101,660,000
101,670,000
Het vs null DMRs
Neurog3 het HMRs
Neurog3 het
Neurog3 null HMRs
Neurog3 null
0.75
0
Nkx6-1
C
D
Scale
chrX :
93,285,000
93,290,000
93,295,000
93,300,000
Neurog3 Het HMRs
Neurog3 Het
Arx
2 kb
93,287,000
93,289,000

Figure S7

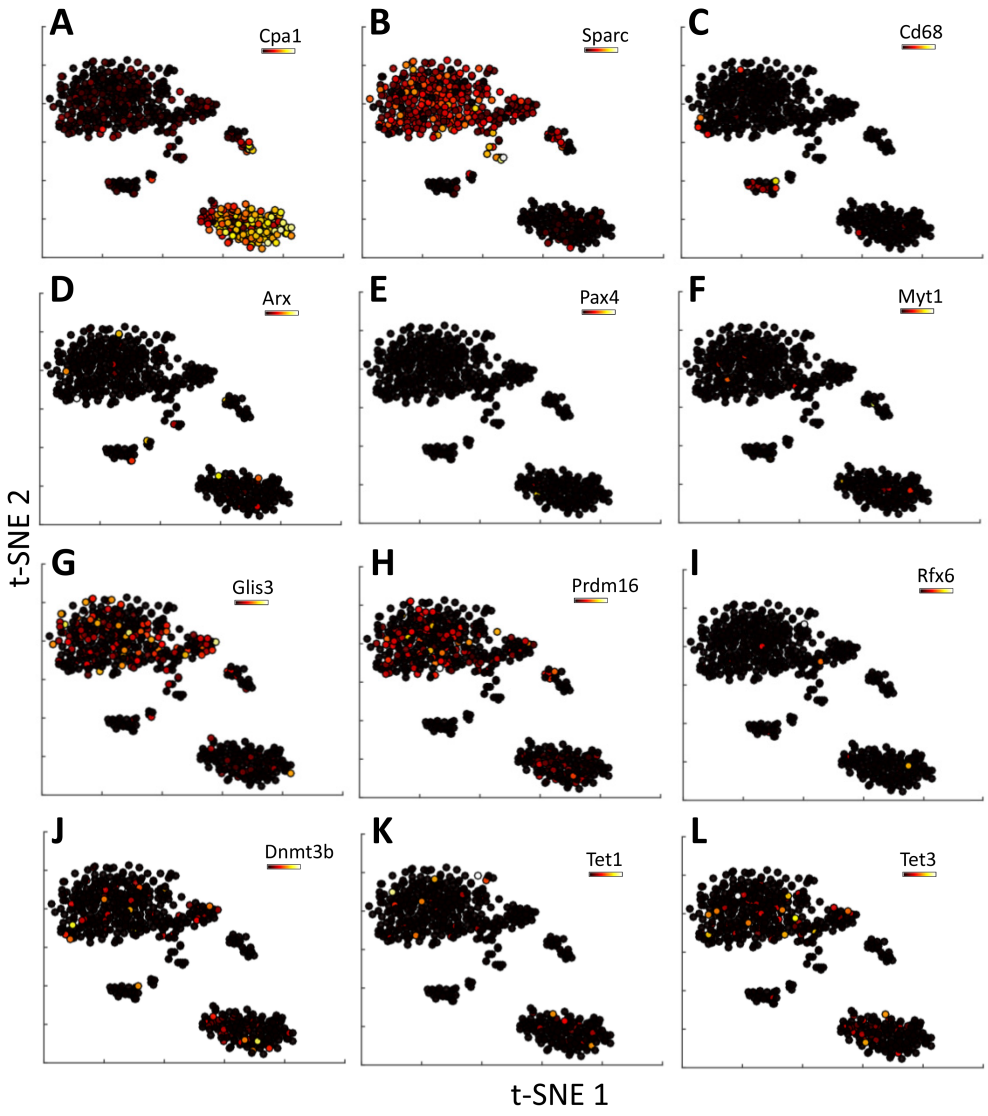
A
Cpa1
B
Sparc
C
Cd68
D
Arx
E
Pax4
F
Myt1
G
Glis3
H
Prdm16
I
Rfx6
J
Dnmt3b
K
Tet1
L
Tet3
t-SNE 2
t-SNE 1

Supplementary Table 3

cell number quantifications used in each figure graph

Figure 1H	beta-trajectory	Cell #	16	13	24	37	47	19	22	20	6	9	4	2	2	1	4	3	2	1	2	3	5	9	3	4	5	6	37
		Expression	0.32	0	0.485	0.2	0.189	0.153	0.532	0.119	0.565	0.0556	0.211	0	0	0	0	0	0.2	0	0	0	0.2	0.1	0	0	0.4	0.2	0.2
	alpha-trajectory	Cell #	7	4	9	5	11	10	6	7	13	10	6	3	3	2	6	12											
		Expression	0	0	0.108	0	0.271	0.501	0	0	0	0	0.272	0	0.3	0.2	0	0.1											

Figure 2B5

mouse #	ins+tDT+	Ins+	Gcg+ tDT+	Gcg+	SS+ tDT+	SS+	PP+ tDT+	PP+	mice #	Horm+ RFP+	Horm+
#11	1176	2222	316	2500	155	404	106	383	#1	127	432
#4	1114	2320	215	2013	102	247	78	387	#2	109	317
#1	703	1341	245	796	154	392	62	226	#3	152	390
#2	694	1387	159	1207	84	231	70	236	#4	73	221
#3	799	1098	199	1123	73	242	94	247	#5	129	233
#12	658	1179	187	1108	117	347			#6	120	374
#13	616	1123	169	930	97	214			#7	77	201
#14	1017	1612	137	881	79	386			#8	210	529
#22	1818	2956	100	683	113	226			#9	206	514
#23	342	957	160	1075	86	238	100	187			
#33	258	812	272	1268	52	257	64	279			
#34	741	1316	139	896	181	394	150	351			
#15	574	1095	89	897	85	301	40	151			

Figure 2C3

mice #	ins+tDT+	Ins+	Gcg+t DT+	Gcg+	mice #	Gast+t DT+	Gast+	Ghrl+t DT+	Ghrl+
#1	351	768	65	201	#11	30	155	16	216
#2	229	374	73	360	#12	40	112	14	134
#3	568	762	61	352	#13	26	159	19	133
#4	329	792	107	1092	#14	57	192	16	104
#5	260	465	129	840	#15	28	133	13	110
#6	164	332	45	308	#16	38	137	21	92
#7	256	360	34	301	#17			8	114
#8			167	860					

Figure 2D3

mice #	Myt1+Ngn	Ngn3+	mice #	Myt1+N	Ngn3+
control-1	115	243	transge	147	183
control-2	87	186	transge	179	203
control-3	85	206	transge	180	191

Figure

mice #	beta	alpha	mice #	beta	alpha
WT-1	1421	1016	Transg	1622	809
WT-2	1638	1233	Transg	1273	987
WT-3	1091	908	Transg	1441	892

2E	WT-4	976	930	Transg	1387	731

	cotnrol1		Mutant1		control2		mutant2		contorl3		mutant3	
Figure	alpha	beta	alpha	beta	alpha	beta	alpha	beta	alpha	beta	alph	beta
2F3	358	536	307	370	479	729	565	700	548	871	750	1022

	E12.5					E14.5					
	bud #	alpha	beta	alpha	beta	**bud #**		alpha	beta	alpha	beta
	#1	209	572	143	284		#1	275	909	586	1008
	#2	232	395	167	265		#2	346	667	481	956
	#3	83	351	292	387		#3	112	420	413	549
	#4	285	492	265	446		#4	363	692	404	652
Figure							#5	174	605	562	945
4D		control		AzaC				control		AzaC	

		DNMT1OE			control	
	mice #	alpha	beta	**mice #**	alpha	beta
	1	722	437	1	930	640
	2	548	394	2	322	463
	3	95	78	3	425	441
Figure	4	1324	1157	4	1542	710
4G	5	322	359	5	397	272

		dCas9-TG			Control	
	1	alpha	beta	1	alpha	beta
	2	2508	1902	2	1254	822
	3	1277	749	3	1811	1410
	4	1670	651	4	1593	1222
Figure	5	3562	1603	5	2762	2797
6E3	6	1319	571			

s